FULL PAPER

Dalton
www.rsc.org/dalton

Novel one-dimensional structures and solution behaviour of copper(II) bromide and chloride complexes of a new pentapyridyldiamine ligand †

David G. Lonnon,[a] Donald C. Craig,[a] Stephen B. Colbran *[a] and Paul V. Bernhardt[b]

[a] *School of Chemical Sciences, University of New South Wales, Sydney, NSW 2052, Australia*

[b] *Department of Chemistry, University of Queensland, St Lucia, Brisbane, Queensland, QLD 4072, Australia*

Received 25th November 2003, Accepted 23rd January 2004
First published as an Advance Article on the web 10th February 2004

Copper(II) bromide and chloride complexes of the new heptadentate ligand 2,6-bis(bis(2-pyridylmethyl)amino)-methylpyridine (L) have been prepared. For the bromide complexes, chains of novel, approximately C_2-symmetric, chiral $[Cu_2(L)Br_2]^{2+}$ 'wedge-shaped' tectons are found. The links between the dicopper tectons and the overall chirality and packing of the chains are dictated by the bromide ion content, not the counter anion. In contrast, the chloride complexes exhibit linked asymmetric $[Cu_2(L)Cl_3]^+$ tectons with distinct N_3CuCl_2 and N_4CuCl_2 centres in the solid. The overall structures of the dicopper bromide and chloride units persist in solution irrespective of the halide. The redox chemistry of the various species is also described.

Introduction

Polypyridylamine ligands exhibit a coordination chemistry both rich and diverse. Two examples with widely investigated coordination chemistries are tetradentate tris(2-pyridylmethyl)-amine (TPA) and tridentate bis(2-pyridylmethyl)amine (BPA). Transition metal complexes with BPA and TPA donor domains catalyse a raft of useful chemical transformations such as atom transfer radical polymerisation,[1] hydrolysis,[2–4] organic hydroxylation,[5–8] oxidations of organic substrates by oxygen, peroxide, or superoxide,[9–16] including oxidation of wood pulp,[17,18] transesterification,[19,20] reductive coupling,[21] and the selective oxidative cleavage of DNA.[22–24] Iron and copper complexes incorporating BPA and TPA donor domains are also much used to model aspects of the structure and function of non-heme iron and copper proteins, especially those which bind and activate dioxygen.[25–37]

Recently investigations of monomeric BPA and TPA complexes have been extended to oligometallic species that incorporate two or more BPA or TPA donor domains.[14,22–24,27,31,38–42] It is found that bimetallic or metallo-oligomers may exhibit reactivity over and above that of the corresponding monomeric BPA or TPA complex. For example, dioxygen activation and catalytic oxidation activity may be enhanced when the two transition metals are capable of simultaneously binding oxygen.

Surprisingly, dimeric complexes bridged by a ligand incorporating both BPA and TPA donor sets had not been reported prior to this work. Herein are described the synthesis and copper(II) halide complexes of the new ligand 2,6-bis(bis-(2-pyridylmethyl)amino)methylpyridine (L),[43] which may be thought of as being constructed from directly linked BPA and TPA donor sets. This investigation of the copper coordination chemistry of L was undertaken as a prelude to studies of the oxygen chemistry and catalytic potential of its (di)copper complexes. Crystalline complexes with novel one-dimensional structures were obtained and the solution and redox behaviours of the various species characterised.

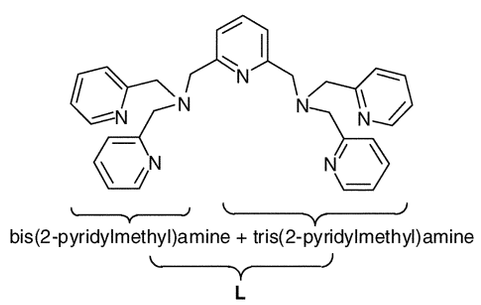

Results

Preparations

Ligand synthesis. L was obtained in high yield (~90–95%) from 2,6-di(bromomethyl)pyridine[44] with two equivalents of bis(2-pyridylmethyl)amine[45] and excess K_2CO_3 in acetonitrile at ambient temperature for 2 h. Smaller scale (<1 g) preparations sometimes gave bromide-containing salts of the ligand, that is L·*n*(MBr). The nature of M^+ was not determined but presumably is H^+ or K^+ carried through from the synthesis.

Copper bromide complexes. Five (bromo)copper(II) complexes were prepared, namely $[Cu_2(L)Br_2][BF_4]_2$, $[Cu_2(L)Br_2](ClO_4)_2$, $[Cu_2(L)Br_3](ClO_4)$, $[Cu_2(L)Br_3]_2[Cu_2Br_4]$ and $[Cu_2(L)Br_3]Br$. These five complexes, as listed, have increasing bromide-to-copper (Br : Cu) ratios: 2 : 2, 2 : 2, 3 : 2, 3.3 : 2 and 4 : 2, respectively.

The first two of these dicopper complexes are 'dibromides'. Mixing L·*n*(MBr) and two equivalents of $Cu[BF_4]_2$ in acetonitrile followed by vapour diffusion of diethyl ether gave crystalline, blue $[Cu_2(L)Br_2][BF_4]_2$. The second 'dibromide' complex resulted from an attempt to form a mixed copper–zinc dimer: according to literature precedents[46–49] one equivalent of each of L·*n*(MBr), $Cu(ClO_4)_2$ and $Zn(ClO_4)_2$ were mixed in acetonitrile–methanol (1 : 3) and the solution set aside under a diethyl ether atmosphere – blue crystalline blocks of $[Cu_2(L)Br_2](ClO_4)_2$ grew. ICP-AES analysis of the crystals reveal the Cu : Zn ratio is at least 40 : 1, which is within the margin of error for 'pure' (di)copper complexes, and the spectroscopic data for both 'dibromide' complexes in solution are identical. We conclude the conditions employed favour deposition of the dicopper complex.

† Electronic supplementary information (ESI) available: Table S1: Selected bands from FTIR spectra of solid-state species in KBr disks. Table S2: UV-Vis-NIR spectroscopic data. Fig. S1: Views of the crystal structure of $[Cu_2(L)Br_3]_2[Cu_2Br_4]$, illustrating: (a) the chains of bromide-bridged $[Cu_2(L)Br_2]^{2+}$ tectons and interspersed $[Cu_2Br_4]^{2-}$ counter ions; (b) the packing of the chains and $[Cu_2Br_4]^{2-}$ counter ions. See http://www.rsc.org/suppdata/dt/b3/b315202b/

DOI: 10.1039/b315202b

The other complexes are 'tribromides' and were obtained starting from copper(II) bromide. Recrystallisation of the blue solid obtained from an acetonitrile–methanol solution containing two equivalents of $CuBr_2$, L·*n*(MBr) and excess $LiClO_4$ from acetonitrile–diethyl ether afforded blue crystals of $[Cu_2(L)Br_3](ClO_4)$. Green, microcrystalline $[Cu_2(L)Br_3]Br$ was obtained from reaction of L with two equivalents of $CuBr_2$ in acetonitrile–methanol (2 : 1) under a diethyl ether atmosphere. Likewise green crystals of $[Cu_2(L)Br_3]_2[Cu_2Br_4]$, all of the same habit, grew from a solution of L and two equivalents of $CuBr_2$ in methanol set aside under a diethyl ether atmosphere.

Copper(II) chloride complexes. Addition of diethyl ether to a solution of L with two equivalents of $CuCl_2$ in ethanol precipitated a blue powder that afforded blue prisms of $[Cu_2(L)Cl_3]Cl$ when recrystallised from acetonitrile under a diethyl ether atmosphere. If an excess of $K[PF_6]$ was added prior to the precipitation with diethyl ether, microcrystalline $[Cu_2(L)Cl_3][PF_6]$ resulted.

Solid-state properties

IR, UV-Vis-NIR and EPR Spectroscopies. The FTIR spectrum of L exhibits pyridyl ring deformation bands at 1587 and 1566 cm^{-1}. In the solid complexes, the pyridyl ring deformation bands are at 1607–1609 and 1570–1571 cm^{-1} (see ESI †). The shift in the ν_1 band is diagnostic for coordination of all pyridyl rings to copper.[30,50] Thus, all complexes have fully metal-bound pyridyl donor sets.

In the UV-Vis-NIR solid-state spectra, all dicopper complexes exhibit a single broad d–d band, at 658 and 691 nm for the 'dibromides' $[Cu_2(L)Br_2](ClO_4)_2$ and $[Cu_2(L)Br_2][BF_4]_2$, at 678, 653 and 652 nm for the 'tribromides' $[Cu_2(L)Br_3](ClO_4)$, $[Cu_2(L)Br_3]_2[Cu_2Br_4]$ and $[Cu_2(L)Br_3]Br$ and at 614 and 593 nm for the 'trichlorides' $[Cu_2(L)Cl_3]Cl$ and $[Cu_2(L)Cl_3][PF_6]$. The different band energies for the various salts of the same cation suggest the counter-anions impose different packing environments and so influence the electronic properties of the copper centres.

The powder X-band EPR spectra of $[Cu_2(L)Br_2][BF_4]_2$ and $[Cu_2(L)Br_3]Br$ exhibit a broad isotropic peak at g ~2.12, whereas the spectra for $[Cu_2(L)Br_2](ClO_4)_2$, $[Cu_2(L)Br_3](ClO_4)$ and $[Cu_2(L)Br_3]_2[Cu_2Br_4]$ are better resolved and axial with $g_{||}$ ~2.20 and $g_{\perp}$ ~2.07. Likewise, the powder spectra of $[Cu_2(L)Cl_3]Cl$ and $[Cu_2(L)Cl_3][PF_6]$ also appear axial with $g_{||} \sim 2.22$ and $g_{\perp} \sim 2.04$. Each spectrum is consistent with $d_{x^2-y^2}$ ground states for tetragonal copper(II) centres corresponding to axially elongated octahedral or square planar geometries. The half-field regions in the spectra were completely clear of signals.

Crystallography

Crystal structures were obtained for one 'dibromide' complex, $[Cu_2(L)Br_2](ClO_4)_2·CH_3CN$, two 'tribromide' complexes, $[Cu_2(L)Br_3](ClO_4)$ and $[Cu_2(L)Br_3]_2[Cu_2Br_4]$, and one 'trichloride' species, $[Cu_2(L)Cl_3]Cl$, Figs. 1–4 and Table 1.

Dicopper(II) bromide complexes of L

The dibromodicopper(II) 'wedge'. Common to the three structures are chiral, wedge-shaped $[Cu_2(L)Br_2]^{2+}$ tectons with approximate C_2-symmetry, Fig. 1 and Table 1. Within each 'wedge' ligand L bridges two copper(II) ions, wrapping about these either left- or right-handedly so that two outer pyridines form an 'offset-π-stack' with the central pyridine ring. The π-stacked pyridine rings are splayed apart, Fig. 1, and the mean distance between the ring centroids is 3.6 Å. The two copper(II) centres within each wedge are separated by 4.80–5.05 Å (the Cu ··· Cu′ separation) and are 'turned' by ~128° (the Br_{eq}–Cu ··· Cu′–Br'_{eq} dihedral angle) with respect to each other, and it is the twist in L to accomplish this that renders each

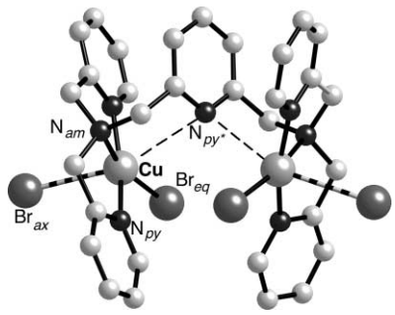

Fig. 1 View of the wedge-shaped $[Cu_2(L)Br_2]^{2+}$ tecton (from the crystal structure of $[Cu_2(L)Br_2](ClO_4)_2·CH_3CN$), also showing the positioning of the axial semibonding bromides; H-atoms are omitted for clarity.

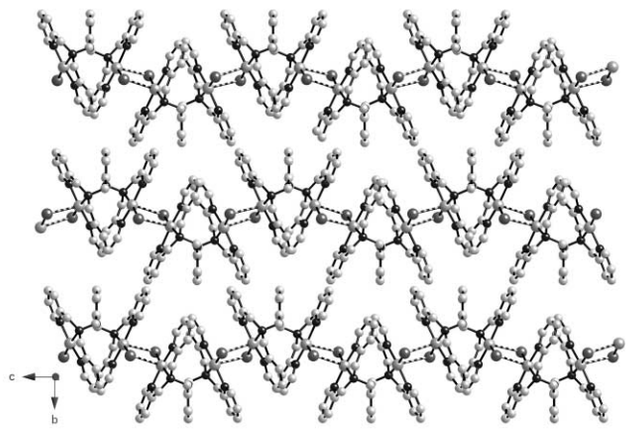

(a)

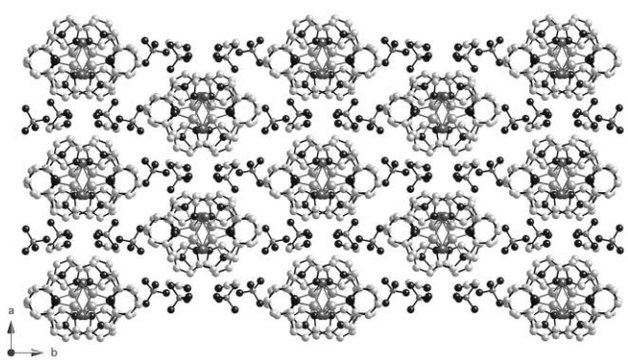

(b)

Fig. 2 Views of the crystal structure of $[Cu_2(L)Br_2](ClO_4)_2·CH_3CN$, illustrating: (a) the chains of directly linked $[Cu_2(L)Br_2]^{2+}$ tectons; (b) the packing of the chains, also showing the positioning of the two perchlorate ions (one is 2 : 1 disordered over two sites; only the major site is depicted) and the lattice acetonitrile; H-atoms are omitted for clarity.

cation chiral. Each copper(II) ion is bound at normal bond lengths by the two pyridine and the amine donors of a di(pyridylmethyl)amine unit and, to complete the equatorial donor set, an ancillary bromide ligand. In the 'axial' positions about each copper are the central pyridine (py*) of L at long Cu ··· N_{py*} distances of 2.88–3.11 Å and a bromide at 2.88–3.08 Å, which is from the adjacent wedge in the 'dibromide' complex, $[Cu_2(L)Br_2](ClO_4)_2·CH_3CN$, and is a 'weakly-bridging' bromide ion in the 'tribromide' complexes, $[Cu_2(L)Br_3](ClO_4)$ and $[Cu_2(L)Br_3]_2[Cu_2Br_4]$, *vide infra*. The long Cu ··· N_{py*} 'axial' distances and the Cu ··· N_{py*} ··· Cu′ angles of ~112–117° suggest the Cu ··· N_{py*} interaction is non-bonding. Although the copper ion and the three equatorial N

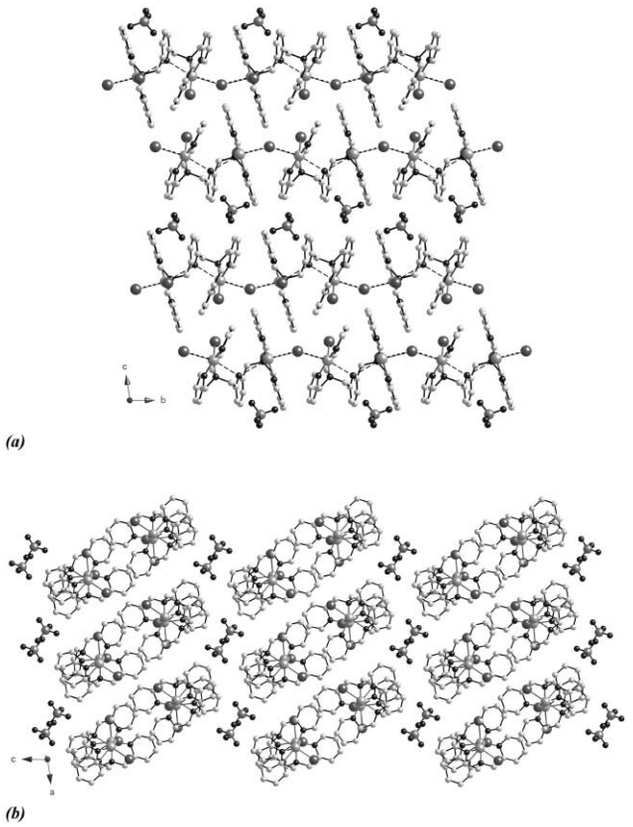

Fig. 3 Views of the crystal structure of $[Cu_2(L)Br_3](ClO_4)$, illustrating: (a) the chains of bromide-bridged $[Cu_2(L)Br_2]^{2+}$ tectons and interspersed ClO_4^- counter ions; (b) the packing of the chains and ClO_4^- counter ions; H-atoms are omitted for clarity.

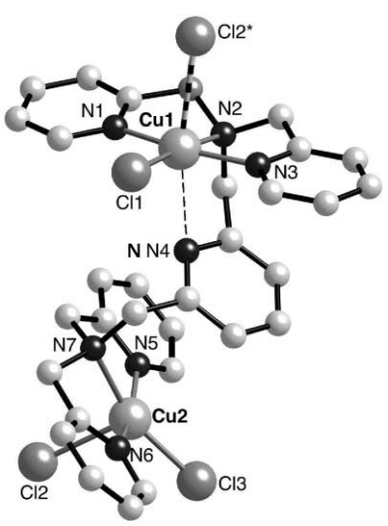

Fig. 4 View of the $[Cu_2(L)Cl_3]^+$ tecton (from the crystal structure of $[Cu_2(L)Cl_3]Cl{\cdot}6H_2O$). Cl2* is the symmetry-related equivalent of Cl2; H-atoms are omitted for clarity. Key bond length (Å) and bond angle (°) data: Cu1–Cl1 2.249(2), Cu1–Cl2 2.774(2), Cu1–N1 1.984(6), Cu1–N2 2.001(6), Cu1–N3 2.059(5), Cu1–N4 2.638(5), Cu2–Cl2 2.550(2), Cu2–Cl3 2.255(2), Cu2–N5 2.012(6), Cu2–N6 2.004(6), Cu2–N7 2.055(5); Cl1–Cu1–N3 174.8(2), N1–Cu1–N2 163.8(2), Cl2–Cu1–N4 166.7(1), Cl3–Cu2–N7 160.6(2), N5–Cu2–N6 161.5(2).

donors lie in a plane, the transoid N_{py}–Cu–N'_{py} angles are acute (~164°) due to constraints imposed by the ligand design. Of note, the equatorial bromide is bent out of the equatorial CuN_3 plane toward N_{py}* by ~10–20° (see the ζ and N_{am}–Cu–Br_{eq} angles, Table 1).

Crystal structure of $[Cu_2(L)Br_2](ClO_4)_2{\cdot}CH_3CN$. In the crystal structure of $[Cu_2(L)Br_2](ClO_4)_2{\cdot}CH_3CN$, each equatorial bromide (Br_{eq}) ligand adopts the axial bromide (Br_{ax}) position of the adjacent wedge. The resultant weak, asymmetric Cu–Br ··· $Cu_{(adjacent\ wedge)}$ bridges link the adjacent $[Cu_2(L)Br_2]^{2+}$ wedges into chains, Fig. 2(a). Neighbouring $[Cu_2(L)Br_2]^{2+}$ wedges are inverted by crystallographic symmetry, so the enantiomers alternate along a given chain. The Cu ··· Cu intramolecular distance in $[Cu_2(L)Br_2]^{2+}$ (4.803 Å) is longer than the closest intermolecular Cu ··· Cu distance (3.674 Å) between neighbouring wedges. Packing of the chains in the crystal is shown in Fig. 2(b). There are no close inter-chain contacts; the shortest inter-chain Cu ··· Cu distance is 12.556 Å. The two ClO_4^- counter ions and the acetonitrile molecule per $[Cu_2(L)Br_2]^{2+}$ wedge are well defined and positioned within the voids between the chains.

Crystal structures of $[Cu_2(L)Br_3](ClO_4)$ and $[Cu_2(L)Br_3]_2[Cu_2Br_4]$. The crystal structures of the two 'tribromide' complexes are remarkably similar. Each is formed by packing pairs of chains in which the $[Cu_2(L)Br_2]^{2+}$ 'wedges' are linked along the *c*-axis by a weakly bridging bromide ion, Fig. 3 and ESI.† Each chain is composed of a single $[Cu_2(L)Br_2]^{2+}$ enantiomer, with the complementary enantiomer forming the other chain of the pair. The Cu ··· Cu distance between adjacent wedges within a chain is ~5.7 Å in both structures. The inter-chain Cu ··· Cu distances between complementary wedges within each pair of chains reveal the chains are slightly closer in $[Cu_2(L)Br_3]_2[Cu_2Br_4]$ (7.808 and 8.084 Å) than in $[Cu_2(L)Br_3](ClO_4)$ (8.978 and 9.528 Å). The closest inter-chain Br ··· Br contact is between an equatorial bromide and its symmetry-related complement and is 4.279 Å for $[Cu_2(L)Br_3]_2[Cu_2Br_4]$ and 4.376 Å for $[Cu_2(L)Br_3](ClO_4)$.

The ClO_4^- and planar $[Cu_2Br_4]^{2-}$ counter-ions lie interspersed between the pairs of chains, *e.g.* Fig. 3 and ESI.† The bond lengths and angles for $[Cu_2Br_4]^{2-}$ are as expected for this dicopper(I) species.[51–55] The closest Cu ··· Cu distances between the pairs of chains are similar in both structures at 8.896 Å parallel to the *a*-axis and 11.953 Å parallel to the *c*-axis for $[Cu_2(L)Br_3](ClO_4)$ compared to 9.084 and 11.961 Å for $[Cu_2(L)Br_3]_2[Cu_2Br_4]$.

Dicopper(II) chloride complex, $[Cu_2(L)Cl_3]Cl{\cdot}6H_2O$

The crystal structure of $[Cu_2(L)Cl_3]Cl{\cdot}6H_2O$ consists of chains of linked asymmetric $[Cu_2(L)Cl_3]^+$ cations, Figs. 4 and 5. The geometry of the Cu1 centre can be described as tetragonally-elongated octahedral, with Cl1 and a BPA moiety equatorially bound and N4 of the central pyridyl ring and Cl2* axially bound at long distances [Cu1 ··· Cl2* 2.774(2) Å and Cu1 ··· N4 2.638(5) Å; N4–Cu1–Cl2* 166.6(2)°]. The mean of the transoid equatorial N2–Cu1–Cl1 [174.8(2)°] and N1–Cu1–N3 [163.8(2)°] angles (2β) is 169.2, indicative of a slight tetrahedral distortion away from ideal planar equatorial geometry (2β is 180° for ideal square planar and 109.5° for ideal tetrahedral geometries). The Cu2 centre is well described as square pyramidal [trigonality index[56] (τ) = 0.0], equatorially bound at 'usual' distances by a BPA moiety and Cl3 and with Cl2 weakly bound in the axial position [Cu2–Cl2 2.550(2) Å].

Figs. 4 and 5(a) illustrate how each $[Cu_2(L)Cl_3]^+$ cation is linked by the weak Cu1 ··· Cl2* [2.774(2) Å] bridge to the adjacent cation, which has opposite chirality. The copper centres in the adjacent $[Cu_2(L)Cl_3]^+$ cations are rotated by ~60° with respect to each other as is revealed by the Cl1–Cu1 ··· Cu1*–Cl1* (60.5°) and Cl3–Cu2 ··· Cu2*–Cl3* (58.8°) dihedral angles. The weak Cu1 ··· Cl2* bridges link the cations into chains which are paired in the crystal and run parallel to the *c*-axis, Fig. 5. The equatorial Cl2 chlorides are directed toward the centre of each pair of chains affording stabilising inter-chain Cl2 ··· Cl2* contacts of 4.2 Å. A series of stabilising intra- and inter-chain C–H ··· Cl close contacts, typically about 2.7 Å for CH ··· Cl and 3.35 Å for HC ··· Cl,

Table 1 Selected bond lengths (Å) and bond angles (°) for the dicopper bromide complexes

	$[Cu_2(L)Br_2](ClO_4)_2{\cdot}CH_3CN$	$[Cu_2(L)Br_3](ClO_4)$	$[Cu_2(L)Br_3]_2[Cu_2Br_4]$[43]
$Cu–Br_{eq}$	2.385(1)	2.404(2)	2.371(2)
	2.387(1)	2.355(2)	2.400(2)
$Cu–Br_{ax}$	3.022(2)	2.900(2)	3.037(2)
	3.037(2)	3.076(2)	2.882(2)
$Cu–N_{py*}$	2.898(8)	3.109(8)	2.883(8)
	2.906(7)	2.833(8)	3.082(8)
$Cu–N_{py}$	2.003(8)	1.982(8)	1.985(8)
	2.016(8)	1.987(7)	2.071(8)
	1.981(8)	1.993(7)	1.985(8)
	2.001(8)	2.023(8)	1.992(8)
$Cu–N_{am}$	2.037(7)	2.068(7)	2.070(8)
	2.051(7)	2.060(7)	2.086(8)
Cu ··· Cu′	4.803	5.055	4.983
$Br_{ax}–Cu–N_{py*}$	156.6(2)	157.2(2)	160.8(2)
	162.4(2)	165.2(2)	159.4(2)
$Br_{eq}–Cu–N_{am}$	172.5(2)	161.3(2)	168.0(2)
	170.2(2)	170.6(2)	162.5(2)
$N_{py}–Cu–N'_{py}$	164.0(4)	163.9(2)	163.5(3)
	164.0(4)	163.7(2)	164.3(4)
$Cu–N_{py*}–Cu'$	111.8	116.5	113.3
ζ[a]	11	10	14
	11	19	19

[a] ζ Is $90 - \theta$, where θ is the angle between the $Cu–Br_{eq}$ bond and the normal to the equatorial CuN_3 best-plane.

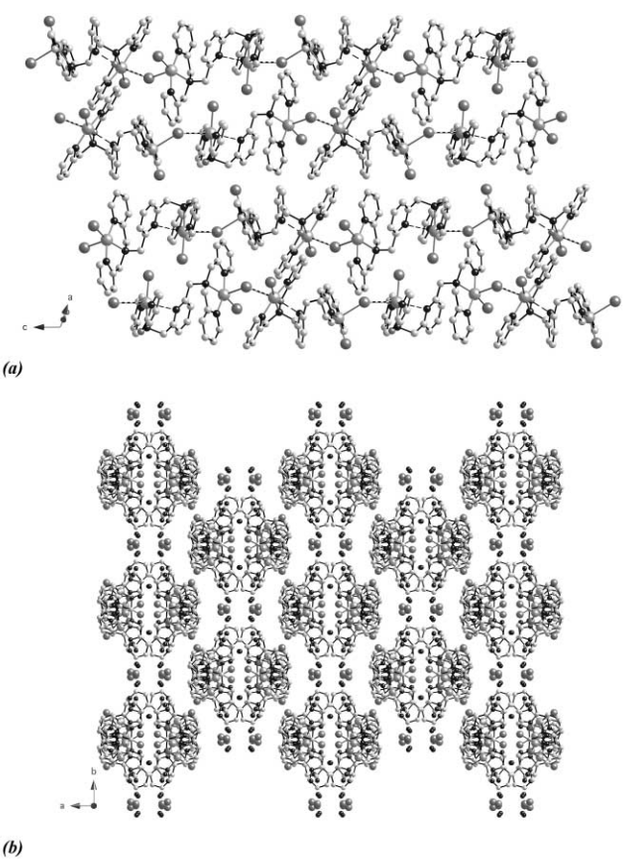

Fig. 5 Views of the crystal structure of $[Cu_2(L)Cl_3]Cl{\cdot}6H_2O$, illustrating: (a) the chains of chloride-bridged $[Cu_2(L)Cl_3]^{2+}$ tectons; (b) the packing of the chains and the Cl^- counter ions (large isolated spheres) and lattice water (small isolated spheres). The chloride ion and three waters are disordered (see Experimental section); both sites for the chloride ion are drawn in the diagram; H-atoms are omitted for clarity.

are also found throughout the structure. The intra-cation Cu1 ··· Cu2 separation is 6.590 Å, the Cu1 ··· Cu2* separation between adjacent cations is 5.069 Å and, within a pair of chains, the closest interchain Cu ··· Cu separation for Cu1 is 7.105 Å and for Cu2 is 7.251 Å. The closest Cu ··· Cu separation between the pairs of chains is 8.160 Å.

Table 2 Molar electrical conductivities (±5%) for the complexes (~10^{-3} M) in acetonitrile and in dimethylformamide solutions

	Λ_M/S cm² mol^{-1}	
Complex	CH_3CN	DMF
$[Cu_2(L)Br_2](ClO_4)_2$	300	135
$[Cu_2(L)Br_2][BF_4]_2$	280	140
$[Cu_2(L)Br_3](ClO_4)$	110	75
$[Cu_2(L)Br_3]_2[Cu_2Br_4]$	275	170
$[Cu_2(L)Br_3]Br$	120	95
$[Cu_2(L)Cl_3]Cl$	160	105
$[Cu_2(L)Cl_3][PF_6]$	130	95
$[(n\text{-}Bu)_4N][PF_6]$	150	80

Solution-state properties

Electrospray mass spectroscopy. The positive-ion ESI-MS spectra of the two dibromides, $[Cu_2(L)Br_2]X_2$ (X^- = BF_4^- or ClO_4^-), exhibit a prominent peak at *m/z* 394 for the $[Cu_2(L)Br_2]^{2+}$ ion (calc. *m/z* 394.3), attesting to this dimeric cation being present in the acetonitrile–water feed solution. The tribromides, $[Cu_2(L)Br_3]Y$ (Y^- = Br^- or ClO_4^-) and $[Cu_2(L)Br_3]_2[Cu_2Br_4]$, exhibit the *m/z* 394 peak and a second prominent peak at *m/z* 868 for the tribromide species $[Cu_2(L)Br_3]^+$ (calc. *m/z* 868.4). $[Cu_2(L)Br_3]Br$ also shows a weak peak at *m/z* 949 for a tetrabromide species, $[Cu_2(L)Br_4 + H]^+$ (calc. 949.3), suggestive for formation of such a species when excess bromide is present in solution. Positive-ion ESI-MS spectra of $[Cu_2(L)Cl_3]Z$ (Z^- = Cl^-, PF_6^-) each show two prominent peaks for $[Cu_2(L)Cl_2]^{2+}$ (*m/z* 350; calc. 349.8) and $[Cu_2(L)Cl_3]^+$ (*m/z* 734; calc. 735.1), respectively. Spectra of $[Cu_2(L)Cl_3]Cl$ also reveal a very low intensity peak for the ion cluster $[Cu_3(L)_2Cl_4]^+$ (*m/z* 1335; calc. 1335.7).

Electrical molar conductivity. Table 2 presents molar electrical conductance values for the complexes in dilute acetonitrile or dimethylformamide solution. These are consistent with $[Cu_2(L)Br_2]X_2$ (X^- = BF_4^- or ClO_4^-) and $[Cu_2(L)Br_3]_2[Cu_2Br_4]$ behaving as 2 : 2 electrolytes and $[Cu_2(L)Br_3]Y$ (Y^- = ClO_4^- or Br^-) as 1 : 1 electrolytes, which is, in turn, indicative for simple dissociation of these salts in solution. Thus solutions of the 'dibromide' salts contain $[Cu_2(L)Br_2(S)_n]^{2+}$ (S = solvent; n = 0–4) dication whereas those of the 'tribromide' salts

predominantly contain the $[Cu_2(L)Br_3(S)_m]^+$ ($m < n$) cation. Likewise, the values for $[Cu_2(L)Cl_3]Z$ ($Z^- = Cl^-$ or $[PF_6]^-$) are indicative for 1 : 1 electrolytes, again suggesting simple dissociation of these salts in solution. The data for $[Cu_2(L)Q_3]Q$ ($Q^- = Cl^-$ or Br^-) imply binding of a fourth halide to the dicopper species is weak (see below).

UV-Vis-NIR spectroscopy. A table of UV-Vis-NIR data for all complexes is presented in the ESI.† In solution, both 'dibromide' complexes exhibit ligand-centred bands below ~400 nm and a strong, symmetrical d–d band at 670 nm (ε_{max}/dm^3 mol^{-1} cm^{-1} 230) in acetonitrile and 690 nm (220) in dimethylformamide ascribed to the d_{xz}, $d_{yz} \longrightarrow d_{x^2-y^2}$ transition for a single species with identical copper centres, *e.g.* Fig. 6(a). Spectra of the 'tribromide' complexes in both acetonitrile and dimethylformamide show ligand-centred bands below ~ 350 nm and a strong band at ~750 nm (ε_{max}/dm^3 mol^{-1} cm^{-1} ~180) corresponding to the d_{xz}, $d_{yz} \longrightarrow d_{x^2-y^2}$ transition with a distinct low energy shoulder at ~940 nm (ε_{max}/dm^3 mol^{-1} cm^{-1} ~120) for the $d_{xy} \longrightarrow d_{x^2-y^2}$ transition, *e.g.* Fig. 6(b). The distinct d–d band energies and profiles clearly reveal the 'dibromides' and 'tribromides' to be different species. UV-Vis-NIR spectra of the two trichloride complexes in dimethylformamide solution exhibit a strong d–d band at ~725 nm (ε_{max}/dm^3 mol^{-1} cm^{-1} ~200) with a shoulder to lower energy at ~930 nm, and a new band, not seen in spectra of the ligand, at ~450 nm. All of these spectra are diagnostic for tetragonal copper(II) centres.

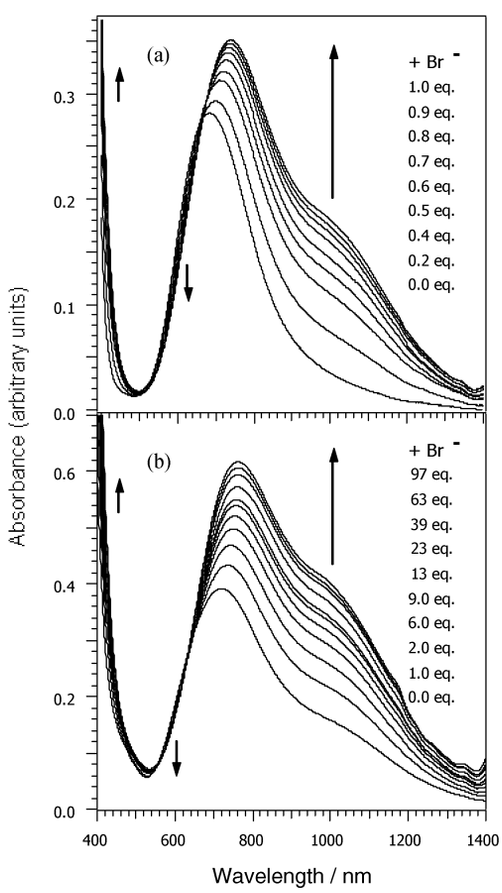

Fig. 6 Incremental Vis-NIR spectral changes for (a) $[Cu_2LBr_2](ClO_4)_2$ and (b) $[Cu_2LBr_3](ClO_4)$ accompanying titrations with bromide ion in dimethylformamide. The equivalents of bromide ion added (as Et_4NBr) are indicated.

EPR spectroscopy. X-Band spectra of the complexes in frozen glasses at 77 K were acquired for all complexes in rapidly frozen acetonitrile, methanol, dimethylformamide and nitromethane solutions (the solution spectra at room temperature are broad and uninformative). Surprisingly the spectra of the 'dibromide' and the 'tribromide' dicopper complexes are all the same, varying only in resolution from one solvent to another. The best-resolved spectra were obtained in nitromethane for the bromides and in methanol for the chlorides. The spectra, *e.g.* Fig. 7 and Table 3, are unlike those of isolated copper(II) centres due to weak dipolar coupling between the two copper(II) centres. No half-field ($\Delta M = 2$) transitions were observed in

Table 3 Spin-Hamiltonian and structural parameters for the complexes from simulations of the frozen solution X-band EPR spectra at 77 K

	$[Cu_2(L)Br_3]ClO_4$[a]	$[Cu_2(L)Cl_3]Cl$[b]
r/Å	4.9	5.7
ξ/°	33	29
τ/°	38	50
η/°	45	45
g_z	2.200	2.230
g_y	2.070	2.025
g_x	2.070	2.025
A_z/G	196	159
A_y/G	41	21
A_x/G	41	21

[a] $MeNO_2$ spectrum. [b] MeOH spectrum.

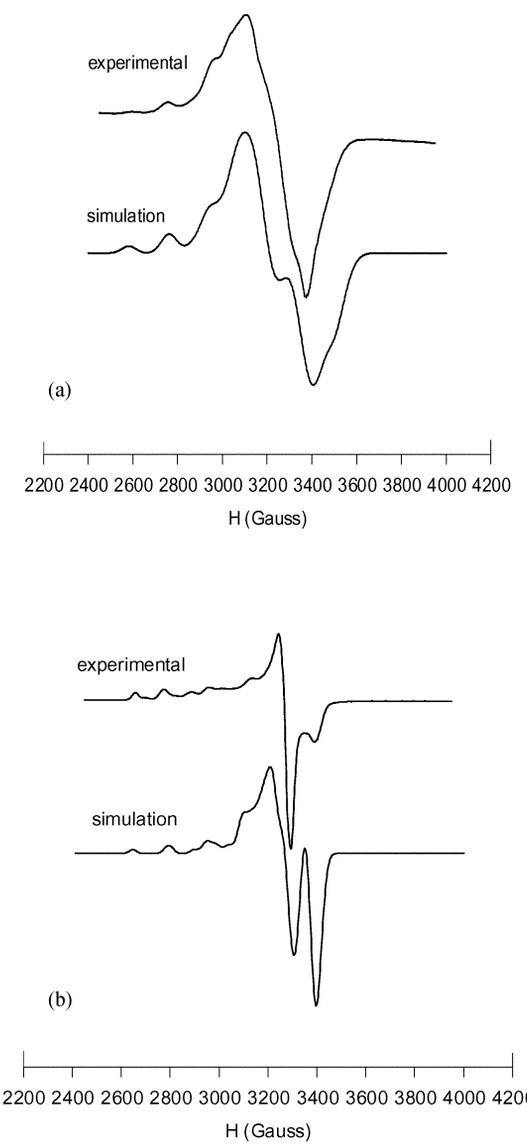

Fig. 7 Experimental and simulated X-band EPR spectra for (a) $[Cu_2(L)Br_3]ClO_4$ in frozen $MeNO_2$ solution and (b) $[Cu_2(L)Cl_3]Cl$ in frozen methanol solution. Conditions: $\nu = 9.52$ GHz, $T = 77$ K.

the spectra, indicating the absence of strong spin-coupling between the copper centres in these dicopper species.[57,58] Spin-Hamiltonian and structural parameters (see Fig. 8) were extracted from spectral simulation, Table 3, and are indicative for tetragonal copper(II) centres ($d_{x^2-y^2}$ ground state). Importantly, the dipole–dipole coupling and, consequently, the appearance of the EPR spectrum is strongly perturbed by the separation (r) of the copper centres (since $\Delta H_{dipolar} \sim 1/r^3$).[59] The simulated xy plane for each copper centre in the bromide dimers closely corresponds to the crystallographic equatorial plane (defined by the copper and the three equatorial nitrogen and one equatorial bromide donors) and the simulated inter-copper distance is 4.9 Å, the same separation as found within the dicopper 'wedges' in the crystal structures (see above). The spectral parameters of the bromide species are thus entirely consistent with the dicopper 'wedge' structure being maintained in solution. The estimated inter-copper separation within the 'trichloride' species is 5.7 Å, much closer than the 6.6 Å inter-copper separation in the crystal structure of $[Cu_2(L)Cl_3]Cl{\cdot}6H_2O$, indicative for a more compact $[Cu_2(L)Cl_3]^+$ cation in solution than in the solid state.

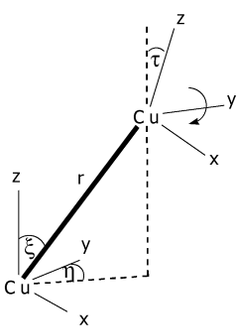

Fig. 8 Definition of distance and angular parameters in EPR simulations.

Bromide ion equilibria. The sequential uptake of bromide ion by $[Cu_2(L)Br_2]^{2+}$ to afford $[Cu_2(L)Br_3]^+$, eqn. (1), and then 'higher' bromide species was studied in dimethylformamide solution.

$$[Cu_2(L)Br_2]^{2+} + Br^- \rightleftarrows [Cu_2(L)Br_3]^+ \qquad (1)$$

Spectra from titrations of $[Cu_2(L)Br_2](ClO_4)_2$ with bromide ion reveal the symmetrical peak at ~670 nm for $[Cu_2(L)Br_3]^+$ is cleanly replaced by the unsymmetrical peak at ~720 nm and distinct shoulder at ~960 nm for $[Cu_2(L)Br_3]^+$, Fig. 6(a). An isosbestic point is observed at 664 nm. Job plots[60] confirm that one bromide anion reacts with one $[Cu_2(L)Br_2]^{2+}$ cation, eqn. (1). The bromide affinity constants $[K_3(Br^-)]$ for eqn. (1) at 298 K were obtained from double reciprocal plots of $1/\Delta A_{900\,nm}$ and $1/[Br^-_{added}]$ using the Benesi–Hildebrand equation,[61] which give $K_3(Br^-)$ values of 1.6×10^3 for $[Cu_2(L)Br_2](ClO_4)_2$ and 2.1×10^3 for $[Cu_2(L)Br_2][BF_4]_2$. The small but reproducible lowering of $K_3(Br^-)$ for the perchlorate complex may indicate greater cation–anion association is this case.[62]

Binding of a fourth bromide to the dicopper centre, eqn. (2), was seen at very high bromide concentrations. As $[Cu_2(L)Br_3]^+$ was titrated with excess bromide, its d–d bands were replaced by a more intense, unsymmetrical peak at 763 nm (ε_{max}/dm^3 mol^{-1} cm^{-1} = 255) with a distinct shoulder at 933 nm (ε_{max}/dm^3 mol^{-1} cm^{-1} = 180) for a $[Cu_2(L)Br_4]$ species; the transformation showed an isosbestic point at 638 nm, Fig. 6(b). After addition of ~200 equivalents of bromide ion, no further change in the spectra was observed. The affinity constant, $K_4(Br^-)$, estimated from these spectra is 2.5×10^2.

$$[Cu_2(L)Br_3]^+ + Br^- \rightleftarrows [Cu_2(L)Br_4] \qquad (2)$$

Interestingly, the frozen-glass (77 K) and room-temperature EPR spectra for solutions of the dibromide or tribromide dicopper species did not change upon addition of bromide ion, however much in excess. The invariance in the EPR spectra of these bromo-dicopper species in a particular solvent, irrespective of the bromide content of the complex and bromide concentration in the solution, suggests all species have a similar structure and that the weak-field axial ligands little perturb the spectra (because noticeably different 'di-', tri- and 'tetra'-bromide EPR spectra would be expected if this were not the case).

Electrochemistry

Cyclic voltammograms (CVs) of the dicopper complexes show a single two-electron process that is electrochemically quasi-reversible ($\Delta E_p \approx 110$–130 mV at 100 mV s^{-1} and increases with scan rate, whereas ΔE_p was ~70 mV for the ferrocenium–ferrocene couple) but with poor chemical reversibility ($i_p^{anodic}/i_p^{cathodic} \approx 0.7$–$0.9$), at −0.46 V for $[Cu_2LBr_2]X_2$ and at −0.62 V for $[Cu_2LCl_3]Z$ (*e.g.* Fig. 9). These two-electron processes are attributed to coincident Cu(II)–Cu(I) couples, which implies that each copper centre in a dimer is electrochemically independent of the other. The Cu(II)–Cu(I) couples were not perturbed by (up to ~50 equiv. of) additional halide ion. This suggests either that the observed Cu(II)–Cu(I) couples are for species with lower halogen ligand content, *e.g.* $[Cu_2LQ_2]^{2+}$ ($Q^- = Br^-$ or Cl^-) and that the extra halo-ligands occupy positions which little affect the copper centres – consistent with axial positioning, see above – and/or that the equilibria between these and species with more halogen ligands, *e.g.* eqns. (1) and (2), are rapid compared to the CV timescale. To positive potentials, the CVs show peaks for the successive oxidations of the halide ion (first to the trihalide anion and then to the halogen[50,63]), the currents of which increased as more of the appropriate halide ion was added (as an anhydrous tetraalkylammonium salt) to the solution.

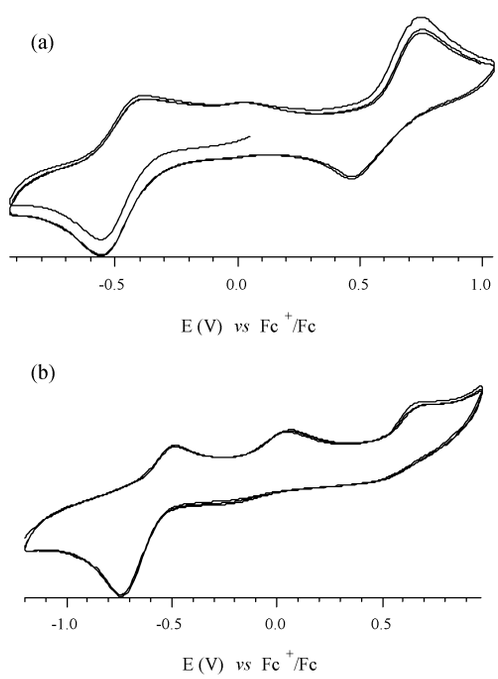

Fig. 9 Cyclic voltammograms for (a) $[Cu_2(L)Br_2][BF_4]_2$ and (b) $[Cu_2(L)Cl_3][PF_6]$. Conditions: ~10^{-3} M complex in dimethylformamide–0.1 M $[(n\text{-}Bu)_4N][PF_6]$; 295 K; 1.0 mm Pt disk working electrode; scan rate = 100 mV s^{-1}.

Discussion

A common tecton is found in the copper bromide structures, the chiral $[Cu_2(L)Br_2]^{2+}$ wedge, in which the central pyridyl

(py*) of L lies almost symmetrically sandwiched between an 'outer' pyridyl from each of the two (BPA)Cu(II) subunits. The available evidence points to the dicopper wedges persisting in solution and to additional bromide binding to each copper ion of a wedge in the 'outward-facing' axial position. For example, the Cu ··· Cu separation within a wedge is ~4.9 Å from the X-ray structures and from simulation of the frozen-solution EPR spectra, and the invariant frozen-solution EPR spectra suggest this separation remains unchanged upon successive additions of bromide ion to afford $[Cu_2(L)Br_3]^+$ then $[Cu_2(L)Br_4]$. The structure of the $[Cu_2(L)Br_2]^{2+}$ wedges places the central pyridyl nitrogen within ~3 Å of both copper ions. A search of the Cambridge crystallographic database revealed fourteen other metal complexes in which the nitrogen of a single pyridyl ring is within 3.1 Å of two metal ions, with the majority being double helicate dimers and all but one, a nickel(II) dimer,[64] are complexes of d^{10} metal ions.[65–76] Thus, the geometry of the $[Cu_2(L)Br_2]^{2+}$ wedges is unusual and these complexes are the first to show a pyridyl nitrogen to within 3.1 Å of two almost symmetrically disposed copper(II) ions.

The copper chloride derivatives contain the $[Cu_2(L)Cl_3]^+$ ion, which appears to adopt a non-symmetrical structure with distinct (BPA)Cu and (TPA)Cu domains. Thus, distinct structures are exhibited by the copper chloride and the copper bromide dimers of L, in the solid-state and in solution. This is not surprising since distortion isomers are typically found for copper(II) complexes as the ancillary ligands and counter ions are changed.[77] It is the structural invariance of the $[Cu_2(L)Br_2]^{2+}$ tecton with counter ion and bromide content that is most remarkable. These results amply illustrate the flexibility of L and suggest fine-tuning of the geometry and properties of the copper centres within complexes of L is possible through judicious choice of ancillary ligands and counter anions.

That the single Cu(II)–Cu(I) couple for the copper chloride or copper bromide dimers is independent of the halide concentration implies the copper dimers vary halide content faster than the CV timescale. The poor chemical reversibility for the Cu(II)–Cu(I) couple may result from loss of the halide ligands upon reduction to afford the Cu(I) dimers. And, lastly, the high potential of the Cu(II)–Cu(I) couple suggests that dicopper(I) species should be readily accessible and that these should exhibit a rich reaction chemistry with dioxygen and its partial reduction products.[29,30,32,34]

Experimental

Bruker AC 300F (300 MHz) or a Bruker DPX 300 (300 MHz) spectrometers were used to record ^1H and $^{13}C\{^1H\}$ NMR spectra. Mass spectra were acquired on a VG Quattro mass spectrometer: electron ionisation (EI) mass spectra were recorded with a 70 eV ionising potential and an ion source temperature of 210 °C and electrospray ionisation (ESI) mass spectra were obtained with a capillary voltage of 4 kV and a cone voltage of 30 V at 60 °C with a feed solvent of 1 : 1 v/v CH_3CN–water (with or without 1% acetic acid as necessary). The peak intensity-averaged mass over the isotopomer envelope of each species is quoted. Elemental analyses for C, H and N were carried out at either the Australian National University Microanalytical Laboratory or at the Campbell Microanalytical Laboratory, University of Otago, New Zealand. Prior to being sent for analysis, samples were dried at 40 °C for 48 h under vacuum (0.2 mmHg) over phosphorus pentoxide. Inductively coupled plasma atomic emission spectroscopy (ICP-AES) analyses for copper and zinc employed a GBC Integra ICP-AES multi-channel instrument. X-Band EPR spectra were recorded on a Bruker EMX 10 spectrometer ($\nu \approx 9.5$ GHz). Simulations were performed with the program DISSIM.[59] Axial spin Hamiltonian parameters ($g_x = g_y \neq g_z$, $A_x = A_y \neq A_z$) are not assumed, merely such a model is the simplest that fully accounts for the characteristically broad frozen solution spectra in which the *x, y* components could not be resolved. IR spectra were recorded using a Mattson Genesis series FTIR spectrometer (1.0 cm^{-1} resolution), and electronic absorption spectra were recorded with a CARY 5 spectrometer. Electrical conductivity measurements were made at 25 °C on ~1×10^{-3} M solutions of the metal complexes using an in-house custom-built electrical conductance meter connected to a Phillips conductivity cell. The conductivities were calibrated against that of the 1 : 1 electrolyte *n*-tetrabutylammonium hexafluorophosphate measured at the same concentration in the same solvent. A computer-controlled Pine bipotentiostat was used for the cyclic voltammetry.[29,30] Except where stated, reagents were purchased from Aldrich and used without further purification.

Preparations

CAUTION: although no problems were encountered during this work, perchlorate salts are potentially explosive materials and appropriate precautions should be taken when handling them.

2,6-Bis(bis(2-pyridylmethyl)amino)methylpyridine (L). To a stirred acetonitrile solution (50 cm^3) of bis(2-pyridylmethyl)-amine[45] (5.40 g, 27.1 mmol) was added an acetonitrile solution (20 cm^3) of 2,6-dibromomethylpyridine[44] (3.60 g, 13.6 mmol) followed by solid K_2CO_3 (4.50 g, 32.4 mmol). Further acetonitrile (70 cm^3) was then added to give a pale yellow suspension. The ^1H NMR spectrum of an aliquot taken after 2 h indicated completion of the reaction, and so the reaction mixture was evaporated to dryness to give an orange oil mixed with white solid. These residues were extracted several times with chloroform (70 cm^3 in total). The chloroform extracts were combined, filtered through a Celite plug, and evaporated under vacuum to produce a tan coloured powder, L (6.26 g, 92%) (Found: C, 72.97, H, 6.00, N, 19.23%. $C_{31}H_{31}N_7 \cdot 0.5H_2O$ requires C, 72.94, H, 6.27, N, 19.22%); δ_H ($CDCl_3$) 8.50 (4 H, d, py), 7.58 (9 H, m, py), 7.41 (2 H, d, py), 7.11 (4 H, t, py), 3.88 (8 H, s, CH_2), 3.86 (4 H, s, CH_2); δ_C ($CDCl_3$) 160.2 (py), 159.4 (py), 149.8 (py), 137.5 (py), 137.1 (py), 123.7 (py), 122.6 (py), 121.8 (py), 60.9 (CH_2); δ_H (d_6-dmso) 8.45 (4 H, d, py), 7.73 (5 H, t, py), 7.58 (4 H, d, py), 7.41 (2 H, d, py), 7.21 (4 H, t, py), 3.78 (8 H, s, CH_2), 3.75 (4 H, s, CH_2); δ_C (d_6-dmso) 159.0 (py), 158.2 (py), 148.8 (py), 137.0 (py), 136.5 (py), 122.5 (py), 122.1 (py), 120.8 (py), 59.5 (CH_2); *m/z* (%) (ESI-MS) 502 (100) $[(L) + H]^+$, 252 (60) $[(L) + 2H]^{2+}$, 524 (20) $[(L) + Na]^+$. ν_{max}/cm^{-1} (KBr) 3426s (OH), 1587s (py), 1566m (py), 1469m (py), 763m (py). Subsequent preparations following the same method, but on a smaller (<1 g) scale, sometimes resulted in the isolation of L·*n*(MBr) (M^+ may be H^+ or K^+; the latter could originate from the K_2CO_3).

$[Cu_2(L)Br_2](ClO_4)_2$. To a solution of L·*n*(MBr) (121 mg) in methanol (4 cm^3) was added a solution of $Cu(ClO_4)_2 \cdot 6H_2O$ (89 mg, 0.24 mmol) in acetonitrile (2 cm^3) followed by a methanolic (2 cm^3) solution of $Zn(ClO_4)_2 \cdot 6H_2O$ (90 mg, 0.24 mmol). The resulting clear green solution was left under a diethyl ether atmosphere for three weeks. Blue crystalline blocks of $[Cu_2(L)Br_2](ClO_4)_2$ formed (38 mg, 32% based on copper) (Found: C, 38.18, H, 3.31, N, 10.87%. $Cu_2C_{31}H_{31}N_7Br_2Cl_2O_8 \cdot CH_3CN$ requires C, 38.53, H, 3.31, N, 10.90%); *m/z* (%) (ESI-MS) 888 (5) $\{[Cu_2(L)Br_2] + (ClO_4)\}^+$, 394 (100) $[Cu_2(L)Br_2]^{2+}$, 314 (30) $[Cu_2(L)]^{2+}$, 282 (30) $[Cu(L)]^{2+}$; ν_{max}/cm^{-1} (KBr) 3431s (OH), 1607s (py), 1571m (py), 1480m (py), 1084s (ClO_4), 767m (py), 722w; λ_{max}/nm (CH_3CN) 290 (ε/dm^3 mol^{-1} cm^{-1} 3700), 320 (3800), 672 (230); (DMF) 290 (3800), 320 (3800), 691 (220); (KBr disc) 658; Λ_M/S cm^2 mol^{-1} (CH_3CN) 300; (DMF) 135; ICP-AES analysis: ratio Cu : Zn = 42.0 : 1.0 (<2.4% Zn).

$[Cu_2(L)Br_2][BF_4]_2$. $Cu[BF_4]_2 \cdot xH_2O$ (Cu(II) 19-22%) (74 mg) in acetonitrile (5 cm^3) was added to L.*n*(MBr) (78 mg,) in

Table 4 Numerical and refinement data for the X-ray crystal structures

	$[Cu_2(L)Br_2](ClO_4)_2\cdot CH_3CN$	$[Cu_2(L)Br_3](ClO_4)$	$[Cu_2(L)Br_3]_2[Cu_2Br_4]$[43]	$[Cu_2(L)Cl_3]Cl\cdot 6H_2O$
Formula (sum)	$C_{33}H_{34}Br_2Cl_2Cu_2N_8O_8$	$C_{31}H_{31}Br_3ClCu_2N_7O_4$	$C_{62}H_{62}Br_{10}Cu_6N_{14}$	$C_{31}H_{43}Cl_4Cu_2N_7O_6$
M	1028.5	967.9	2183.6	878.6
Crystal system	Monoclinic	Triclinic	Triclinic	Monoclinic
Space group	$P2_1/c$	$P\bar{1}$	$P\bar{1}$	$C2/c$
a/Å	11.643(5)	8.896(4)	9.084(3)	25.159(25)
b/Å	22.669(5)	10.771(6)	10.628(4)	16.587(5)
c/Å	15.249(6)	19.092(9)	19.583(7)	21.312(11)
α/°		96.06(3)	100.24(2)	
β/°	102.53(2)	96.45(3)	95.57(3)	113.12(2)
γ/°		103.43(3)	105.44(2)	
V/Å^3	3929(2)	1752(2)	1772(1)	8179(7)
Z	4	2	1	8
μ/cm^{-1} (radiation)	3.294 (Mo-Kα)	4.729 (Mo-Kα)	7.405 (Mo-Kα)	4.122 (Cu-Kα)
Reflections collected	6403	6363	6648	7171
R_{merge} (no. of equiv. reflections)	0.013 (254)	0.023 (203)	0.061 (434)	0.029 (209)
Observed reflections [$I/\sigma(I) > 2$]	3389	3679	3345	4122
No. of parameters	458	410	415	464
Observed reflections/no. parameters	7.4	9.0	8.1	8.9
Final R, R_w [$I/\sigma(I) > 2$]	0.050, 0.070	0.058, 0.068	0.053, 0.058	0.057, 0.079
Goodness-of-fit	1.65	1.83	1.69	1.77
Max., min. peaks in final difference map/e Å^{-3}	0.85, −0.84	1.27, −1.54	1.41, −1.67	1.21, −1.05

acetonitrile (5 cm^3). The clear dark green solution was placed under a diethyl ether atmosphere and produced, after 4 days, a bluish-green powder. This was recrystallised from methanol-acetonitrile (4:1) to afford a blue-green powder, $[Cu_2(L)Br_2][BF_4]_2$ (26 mg, 17%) (Found: C, 38.17, H, 3.41, N, 10.02%. $Cu_2C_{31}H_{31}N_7Br_2B_2F_8\cdot H_2O$ requires C, 37.98, H, 3.37, N, 10.01%); m/z (%) (ESI-MS) 715 (5) $\{[Cu_2(L)] + [BF_4]\}^+$, 651 (15) $\{[Cu(L)] + [BF_4]\}^+$, 583 (10) $[Cu(L)(H_2O)]^+$, 394 (50) $[Cu_2(L)Br_2]^{2+}$, 282 (100) $[Cu(L)]^{2+}$; ν_{max}/cm^{-1} (KBr) 3432s (OH), 1607s (py), 1571m (py), 1478m (py), 1200–1000s (BF_4), 768m (py), 722w; λ_{max}/nm (CH_3CN) 290 (ε/dm^3 mol^{-1} cm^{-1} 3900), 320 (3900), 666 (245); (DMF) 290 (3900), 320 (3900), 685 (230); (KBr disc) 691; Λ_M/S cm^2 mol^{-1} (CH_3CN) 280, (DMF) 140.

$[Cu_2(L)Br_3](ClO_4)$. To a stirred solution of L (120 mg, 0.24 mmol) in methanol (6 cm^3) was added an acetonitrile solution (1 cm^3) of $CuBr_2$ (107 mg, 0.48 mmol). After 15 min, a methanol (2 cm^3) solution of $LiClO_4$ (190 mg, 1.18 mmol) was added and the resulting clear dark green solution placed under a diethyl ether atmosphere. After 4 days, the green crystalline product was collected by filtration, washed with cold methanol and dried under vacuum (102 mg, 44%) (Found: C, 37.59, H, 3.32, N, 9.87%. $Cu_2C_{31}H_{31}N_7Br_3ClO_4$ requires C, 37.76, H, 3.35, N, 9.95%); m/z (%) (ESI-MS) 888 (5) $\{[Cu_2(L)Br_2] + (ClO_4)\}^+$, 868 (10) $[Cu_2(L)Br_3]^+$, 394 (100) $[Cu_2(L)Br_2]^{2+}$, 314 (20) $[Cu_2(L)]^{2+}$, 282 (10) $[Cu(L)]^{2+}$; ν_{max}/cm^{-1} (KBr) 3422s (OH), 1609s (py), 1570m (py), 1477m (py), 1084s (ClO_4), 769m (py), 721w; λ_{max}/nm (CH_3CN) 290 (ε/dm^3 mol^{-1} cm^{-1} 3700), 320 (3700), 741 (340), 934 sh (205); (DMF) 290 (3700), 320 (3700), 716 (160), 975 sh (60); (CH_3NO_2) 707 (160), 960 sh (70); (KBr disc) 678; Λ_M/S cm^2 mol^{-1} (CH_3CN) 110, (DMF) 75.

$[Cu_2(L)Br_3]_2[Cu_2Br_4]$. To L (95 mg, 0.19 mmol) in methanol (4 cm^3) was added $CuBr_2$ (85 mg, 0.38 mmol) in methanol (4 cm^3). A brown precipitate (29 mg) formed and was collected by filtration and dried under vacuum. This material proved to be insoluble in organic solvents and in water and was not further characterised. The filtrate was evaporated to half its original volume and placed under a diethyl ether atmosphere. Small green crystals of X-ray analysis quality formed (12 mg, 9% relative to copper) (Found: C, 34.07, H, 3.10, N, 9.05%. $Cu_6C_{62}H_{62}N_{14}Br_{10}$ requires C, 34.09, H, 2.84, N, 8.98%); m/z (%) (ESI-MS) 868 (10) $[Cu_2(L)Br_3]^+$, 708 (15) $[Cu_2(L)Br]^+$, 394 (20) $[Cu_2(L)Br_2]^{2+}$, 354 (65) $[Cu_2(L)Br]^{2+}$, 314 (100) $[Cu_2(L)]^{+2}$; 282 (90) $[Cu(L)]^{2+}$; ν_{max}/cm^{-1} (KBr) 3459s (OH), 1607s (py), 1571m (py), 1478m (py), 768m (py), 722w; λ_{max}/nm (CH_3CN) 290 (ε/dm^3 mol^{-1} cm^{-1} 4000), 320 (3900), 751 (775), 942 sh (495); (DMF) 290 (4000), 320 (4000), 729 (510), 948 sh (225); (CH_3NO_2) 746 (615), 915 sh (310); (KBr disc) 653; Λ_M/S cm^2 mol^{-1} (CH_3CN) 275, (DMF) 170.

$[Cu_2(L)Br_3]Br$. To an orange solution of L·n(MBr) (100 mg) in methanol (5 cm^3), $CuBr_2$ (89 mg, 0.40 mmol) in methanol (5 cm^3) was added. A brown intractable powder (34 mg) formed and was removed by filtration. The filtrate was evaporated to dryness, then redissolved in methanol–acetonitrile (2 : 1) and placed under a diethyl ether atmosphere. A green microcrystalline solid precipitated and was collected by filtration and dried under vacuum (62 mg, 33% based on copper) (Found: C, 36.75, H, 3.50, N, 9.70%. $Cu_2C_{31}H_{31}N_7Br_4\cdot 3H_2O$ requires C, 37.14, H, 3.69, N, 9.78%); m/z (%) (ESI-MS) 949 (5) $[Cu_2(L)Br_4 + H]^+$ or $\{[Cu_2(L)Br_3] + HBr\}^+$, 867 (65) $[Cu_2(L)Br_3]^+$, 786 (20) $[Cu_2(L)Br_2]^{2+}$, 708 (15) $[Cu_2(L)Br]^+$; 394 (100) $[Cu(L)Br_2]^{2+}$, 354 (20) $[Cu_2(L)Br]^{2+}$; ν_{max}/cm^{-1} (KBr) 3434s (OH), 1607s (py), 1571m (py), 1478m (py), 768m (py), 723w; λ_{max}/nm (CH_3CN) 290 (ε/dm^3 mol^{-1} cm^{-1} 3900), 320 (3900), 758 (365), 932 sh (250); (DMF) 290 (3900), 320 (3800), 733 (180), 954 sh (100); (KBr disc) 653; Λ_M/S cm^2 mol^{-1} (CH_3CN) 120, (DMF) 95.

$[Cu_2(L)Cl_3]Cl$. $CuCl_2$ (57 mg, 0.42 mmol) and L (104 mg, 0.21 mmol) were mixed in ethanol (20 cm^3). After 18 h, no solid had formed. The resulting clear dark green solution was then reduced in volume by half and added to dry diethyl ether (5 cm^3). A blue–green precipitate formed that was collected by filtration and washed with ethanol (20 cm^3) to give $[Cu_2(L)Cl_3]Cl$ (121 mg, 76%). A portion of this solid was recrystallised from acetonitrile–diethyl ether to give blue crystals of quality suitable for X-ray analysis. All data obtained from the powder and the crystals are identical (Found: C, 44.30, H, 4.25, N, 11.56%. $Cu_2C_{31}H_{31}N_7Cl_4\cdot 4H_2O$ requires C, 44.19, H, 4.63, N, 11.60%); m/z (%) (ESI-MS) 1335 (5) $[Cu_3(L)_2Cl_4]^+$, 1093 (5), 977 (5), 734 (20) $[Cu_2(L)Cl_3]^+$, 350 (100) $[Cu_2(L)Cl_2]^{2+}$; ν_{max}/cm^{-1} (KBr) 3433s (OH), 1607s (py), 1571m (py), 1478m (py), 768m (py), 722w; λ_{max}/nm (CH_3CN) 290 (ε/dm^3 mol^{-1} cm^{-1} 3350), 320 (3500), 452 sh (260), 691 (185); (DMF) 290 (3600), 320 (3600), 451 sh (230), 719 (170), 920 sh (115); (CH_3OH) 290 (3550), 320 (3500), 450 sh (310), 719 (165), 900 sh (105); (KBr disc) 614; Λ_M/S cm^2 mol^{-1} (CH_3CN) 160, (DMF) 105.

$[Cu_2(L)Cl_3][PF_6]$. $CuCl_2$ (54 mg, 0.40 mmol) was added to L (100 mg, 0.20 mmol) in ethanol (20 cm^3) and the clear dark green solution stirred for 20 min. A green solid precipitated as $K[PF_6]$ (100 mg) in ethanol (2 cm^3) was dropwise added. This was filtered off and dried under vacuum to give $[Cu_2(L)Cl_3][PF_6]$ (80 mg, 46%) (Found: C, 39.19, H, 3.56, N, 10.26%. $Cu_2C_{31}H_{31}N_7Cl_3PF_6 \cdot 3H_2O$ requires C, 39.65, H, 3.96, N, 10.50%); *m*/*z* (%) (ESI-MS) 844 (20) $\{[Cu_2(L)Cl_2] + [PF_6]\}^+$, 734 (5) $[Cu_2(L)Cl_3]^+$, 350 (100) $[Cu_2(L)Cl_2]^{2+}$; ν_{max}/cm^{-1} (KBr) 3435s (OH), 1607s (py), 1571m (py), 1478m (py), 837s (PF_6), 768m (py), 721w; λ_{max}/nm (CH_3CN) 290 ($\varepsilon/dm^3\ mol^{-1}\ cm^{-1}$ 3600), 320 (3600), 740 (285), 932 sh (170); (DMF) 290 (3600), 320 (3600), 733 (235), 952 sh (115); (CH_3NO_2) 702 (255) 915 sh (130); (KBr disc) 593; $\Lambda_M/S\ cm^2\ mol^{-1}$ (CH_3CN) 131, (DMF) 96.

Crystallography

Relevant crystal, data collection and refinement data are summarised in Table 4. For $[Cu_2(L)Cl_3]Cl \cdot 6H_2O$, the chloride ion is 1 : 1 disordered over two sites with two waters that, in turn, show half occupancy of two further sites. A third water also exhibits 1 : 1 disorder. The Cl/O (water) atoms were refined using mixed scattering factors constrained to give the correct proportion of Cl in the compound and the correct O (water) to fit the observed electron density.

CCDC reference numbers 225104–225107.

See http://www.rsc.org/suppdata/dt/b3/b315202b/ for crystallographic data in CIF or other electronic format.

Acknowledgements

This research was supported from UNSW Goldstar and Faculty Research Grants.

References

1 K. Matyjaszewski, B. Goebelt, H.-J. Paik and C. P. Horwitz, *Macromolecules*, 2001, **34**, 430.
2 M. J. Young, D. Wahnon, R. C. Hynes and J. Chin, *J. Am. Chem. Soc.*, 1995, **117**, 9441.
3 S. T. Frey, N. N. Murthy, S. T. Weintraub, L. K. Thompson and K. D. Karlin, *Inorg. Chem.*, 1997, **36**, 956.
4 Y. Gultneh, A. R. Khan, D. Blaise, S. Chaudhry, B. Ahvazi, B. B. Marvey and R. J. Butcher, *J. Inorg. Biochem.*, 1999, **75**, 7.
5 R. Y. N. Ho, L. Que, Jr., G. Roelfes, B. L. Feringa, R. Hermant and R. Hage, *Chem. Commun.*, 1999, 2161.
6 J. Y. Ryu, J. Kim, M. Costas, K. Chen, W. Nam and L. Que, *Chem. Commun.*, 2002, 1288.
7 M. Fujita, M. Costas and L. Que, *J. Am. Chem. Soc.*, 2003, **125**, 9912.
8 M. P. Jensen, S. J. Lange, M. P. Mehn, E. L. Que and L. Que, *J. Am. Chem. Soc.*, 2003, **125**, 2113.
9 M. R. Malachowski, H. B. Huynh, L. J. Tomlinson, R. S. Kelly and J. W. F. Jun, *J. Chem. Soc., Dalton Trans.*, 1995, 31.
10 J. H. Kim, C. Kim, R. G. Harrison, E. C. Wilkinson and L. Que, *J. Mol. Catal. A.*, 1997, **117**, 83.
11 K. Chen and L. Que, *J. Am. Chem. Soc.*, 2001, **123**, 6327.
12 H. V. Obias, Y. Lin, N. N. Murthy, E. Pidcock, E. I. Solomon, M. Ralle, N. J. Blackburn, Y. M. Neuhold, A. D. Zuberbuhler and K. D. Karlin, *J. Am. Chem. Soc.*, 1998, **120**, 12960.
13 M. Costas and A. Llobet, *J. Mol. Catal. A.*, 1999, **142**, 113.
14 S. E. Watkins, D. C. Craig and S. B. Colbran, *J. Chem. Soc., Dalton Trans.*, 2002, 2423.
15 K. Chen, M. Costas and L. Que, *J. Chem. Soc., Dalton Trans.*, 2002, 672.
16 M. C. Mimmi, M. Gullotti, L. Santagostini, A. Saladino, L. Casella, E. Monzani and R. Pagliarin, *J. Mol. Catal. A.*, 2003, **204**, 381.
17 T. Tzedakis, *Electrochim. Acta*, 2000, **46**, 99.
18 T. Tzedakis, Y. Benzada and M. Comtat, *Ind. Eng. Chem. Res.*, 2001, **40**, 3435.
19 M. Ito, K. Sakai, T. Tsubomura and Y. S. Takita, *Bull. Chem. Soc. Jpn.*, 1999, **72**, 239.
20 M. Ito, H. Kawano, T. Takeuchi and Y. Takita, *Chem. Lett.*, 2000, 372.
21 R. R. Jacobson, Z. Tyeklar and K. D. Karlin, *Inorg. Chim. Acta*, 1991, **181**, 111.
22 K. J. Humphreys, K. D. Karlin and S. E. Rokita, *J. Am. Chem. Soc.*, 2001, **123**, 5588.
23 K. J. Humphreys, K. D. Karlin and S. E. Rokita, *J. Am. Chem. Soc.*, 2002, **124**, 6009.
24 K. J. Humphreys, K. D. Karlin and S. E. Rokita, *J. Am. Chem. Soc.*, 2002, **124**, 8055.
25 L. Que and W. B. Tolman, *Angew. Chem., Int. Ed.*, 2002, **41**, 1114.
26 M. H. Lim, J. U. Rohde, A. Stubna, M. R. Bukowski, M. Costas, R. Y. N. Ho, E. Munck, W. Nam and L. Que, *Proc. Natl. Acad. Sci. USA*, 2003, **100**, 3665.
27 J. Kuzelka, S. Mukhopadhyay, B. Spingler and S. J. Lippard, *Inorg. Chem.*, 2003, **42**, 6447.
28 J. U. Rohde, J. H. In, M. H. Lim, W. W. Brennessel, M. R. Bukowski, A. Stubna, E. Munck, W. Nam and L. Que, *Science*, 2003, **299**, 1037.
29 A. J. Evans, S. E. Watkins, D. C. Craig and S. B. Colbran, *J. Chem. Soc., Dalton Trans.*, 2002, 983.
30 Z. C. He, S. B. Colbran and D. C. Craig, *Chem. Eur. J.*, 2003, **9**, 116.
31 C. He, J. L. DuBois, B. Hedman, K. O. Hodgson and S. J. Lippard, *Angew. Chem., Int. Ed.*, 2001, **40**, 1484.
32 K. D. Karlin, S. Kaderli and A. D. Zuberbuhler, *Acc. Chem. Res.*, 1997, **30**, 139.
33 C. X. Zhang, H.-C. Liang, K. J. Humphreys and K. D. Karlin, in *Advances in Catalytic Activation of Dioygen by Metal Complexes*, ed. L. I. Simandi; *Catalysis by Metal Complexes*, ed. B. R. James and P. W. V. M. van Leeuwen, Kluwer, Dordreht, Boston & London, 2003, ch. 2, p. 79.
34 M. Schatz, M. Becker, F. Thaler, F. Hampel, S. Schindler, R. R. Jacobson, Z. Tyeklar, N. N. Murthy, P. Ghosh, Q. Chen, J. Zubieta and K. D. Karlin, *Inorg. Chem.*, 2001, **40**, 2312.
35 H. C. Fry, D. V. Scaltrito, K. D. Karlin and G. J. Meyer, *J. Am. Chem. Soc.*, 2003, **125**, 11866.
36 H. Hayashi, S. Fujinami, S. Nagatomo, S. Ogo, M. Suzuki, A. Uehara, Y. Watanabe and T. Kitagawa, *J. Am. Chem. Soc.*, 2000, **122**, 2124.
37 A. Philibert, F. Thomas, C. Philouze, S. Hamman, E. Saint-Aman and J. L. Pierre, *Chem. Eur. J.*, 2003, **9**, 3803.
38 D.-H. Lee, N. Wei, N. N. Murthy, Z. Tyeklar, K. D. Karlin, S. Kaderli, B. Jung and A. D. Zuberbuehler, *J. Am. Chem. Soc.*, 1995, **117**, 12498.
39 K. D. Karlin, D. H. Lee, S. Kaderli and A. D. Zuberbuhler, *Chem. Commun.*, 1997, 475.
40 C. He and S. J. Lippard, *Inorg. Chem.*, 2000, **39**, 5225.
41 C. Walsdorff, S. O. Park, J. Kim, J. Heo, K. N. Park, J. Oh and K. Kim, *J. Chem. Soc., Dalton Trans.*, 1999, 923.
42 A. Hazell, R. Hazell, C. J. McKenzie and L. P. Nielsen, *Dalton Trans.*, 2003, 2203.
43 For a communication containing part of this work: D. G. Lonnon, D. C. Craig and S. B. Colbran, *Inorg. Chem. Commun.*, 2002, **5**, 958.
44 B. Kaptein, G. Barf, R. M. Kellogg and F. Van Bolhuis, *J. Org. Chem.*, 1990, **55**, 1890.
45 J. K. Romary, J. D. Barger and J. E. Bunds, *Inorg. Chem.*, 1968, **7**, 1142.
46 J. L. Pierre, P. Chautemps, S. M. Refaif, C. G. Beguin, A. Elmarzouki, G. Serratrice, P. Rey and J. Laugier, *Chem. Commun.*, 1994, 1117.
47 J. L. Pierre, P. Chautemps, S. Refaif, C. Beguin, A. Elmarzouki, G. Serratrice, E. Saintaman and P. Rey, *J. Am. Chem. Soc.*, 1995, **117**, 1965.
48 H. Ohtsu, Y. Shimazaki, A. Odani and O. Yamauchi, *Chem. Commun.*, 1999, 2393.
49 H. Ohtsu, Y. Shimazaki, A. Odani, O. Yamauchi, W. Mori, S. Itoh and S. Fukuzumi, *J. Am. Chem. Soc.*, 2000, **122**, 5733.
50 Z. C. He, D. C. Craig and S. B. Colbran, *J. Chem. Soc., Dalton Trans.*, 2002, 4224.
51 B. Le Gall, F. Conan, N. Cosquer, J.-M. Kerbaol, M. M. Kubicki, E. Vigier, Y. Le Mest and J. Sala Pala, *Inorg. Chim. Acta*, 2001, **324**, 300.
52 P. Pyykkoe and F. Mendizabal, *Inorg. Chem.*, 1998, **37**, 3018.
53 S. Andersson and S. Jagner, *Acta Crystallogr., Sect. C*, 1987, **43**, 1089.
54 S. Andersson and S. Jagner, *Acta Chem. Scand., Ser. A*, 1985, **39**, 423.
55 M. Asplund and S. Jagner, *Acta Chem. Scand., Ser. A*, 1984, **38**, 135.
56 A. W. Addison, T. N. Rao, J. Reedijk, J. Van Rijn and G. C. Verschoor, *J. Chem. Soc., Dalton Trans.*, 1984, 1349.
57 J. F. Gibson, in *Electron Spin Resonance*, Specialist Periodical Report, ed. R. O. C. Norman, RSC, London, 1973, vol. 1, p. 163.
58 P. D. W. Boyd, T. D. Smith, J. H. Price and J. R. Pilbrow, *J. Chem. Phys.*, 1972, **56**, 1253.

59 T. D. Smith and J. R. Pilbrow, *Coord. Chem. Rev.*, 1974, **13**, 173.
60 P. Job, *Ann. Chim. (Paris)*, 1928, **9**, 113.
61 K. A. Conners, *Binding Constants: the Measurement of Molecular Stability*, J. Wiley & Sons, London, 1987.
62 J. M. Alia and H. G. M. Edwards, *J. Solution Chem.*, 2000, **29**, 781.
63 B. E. Conway, Y. Phillips and S. Y. Qian, *J. Chem. Soc., Faraday Trans.*, 1995, 283.
64 G. Paolucci, S. Stelluto, S. Sitran, D. Ajo, F. Benetollo, A. Polo and G. Bombieri, *Inorg. Chim. Acta*, 1992, **193**, 57.
65 C. Lorenzini, C. Pelizzi, G. Pelizzi and G. Predieri, *J. Chem. Soc., Dalton Trans.*, 1983, 2155.
66 M. G. B. Drew, A. Lavery, V. McKee and S. M. Nelson, *J. Chem. Soc., Dalton Trans.*, 1985, 1771.
67 C. Piguet, G. Bernardinelli and A. F. Williams, *Inorg. Chem.*, 1989, **28**, 2920.
68 S. bin Silong, J. D. Kildea, W. C. Patalinghug, B. W. Skelton and A. H. White, *Aust. J. Chem.*, 1994, **47**, 1545.
69 A. Bino and N. Cohen, *Inorg. Chim. Acta*, 1993, **210**, 11.
70 K. T. Potts, M. Keshavarz-K, F. S. Tham, H. D. Abruna and C. Arana, *Inorg. Chem.*, 1993, **32**, 4450.
71 G. A. Bowmaker, Effendy, P. J. Harvey, P. C. Healy, B. W. Skelton and A. H. White, *J. Chem. Soc., Dalton Trans.*, 1996, 2459.
72 R.-H. Uang and S.-M. Peng, *Bull. Inst. Chem., Acad. Sin.*, 1996, **43**, 117.
73 E. C. Constable, A. J. Edwards, M. J. Hannon and P. R. Raithby, *Chem. Commun.*, 1994, 1991.
74 E. C. Constable, T. Kulke, G. Baum and D. Fenske, *Chem. Commun.*, 1997, 2043.
75 E. C. Constable, M. S. Khan, M. C. Liptrot, J. Lewis and P. R. Raithby, *Inorg. Chim. Acta*, 1991, **179**, 239.
76 E. C. Constable, C. E. Housecroft and T. Kulke, *Chem. Commun.*, 1998, 2659.
77 B. Murphy and B. Hathaway, *Coord. Chem. Rev.*, 2003, **243**, 237.